Geophysical Research Letters

RESEARCH LETTER
10.1029/2025GL121222

# Ocean Bottom Seismometers Provide Direct Measurements of Pulsed-Structure and Turbulence of Turbidity Currents Overspilling From a Submarine Channel

**Pascal Kunath[1], Hans van Haren[2], and Peter J. Talling[3,4]**

[1]GEOMAR Helmholtz Centre for Ocean Research, Kiel, Germany, [2]Royal Netherlands Institute for Sea Research (NIOZ), Den Burg, The Netherlands, [3]Department of Earth Sciences, Durham University, Durham, UK, [4]Department of Geography, Durham University, Durham, UK

**Key Points:**

- Ocean-bottom seismometers measure highly-pulsed structure and turbulence of submarine channel overspill
- Channel overspill persists for weeks and consists of repeated, short-lived pulses
- Overspill-generated turbulence reaches dissipation rates of order $10^{-6}$–$10^{-5}$ $m^2$ $s^{-3}$, comparable to energetic internal-tide breaking

**Supporting Information:**

Supporting Information may be found in the online version of this article.

**Correspondence to:**

P. Kunath,
pkunath@geomar.de

**Citation:**

Kunath, P., van Haren, H., & Talling, P. J. (2026). Ocean bottom seismometers provide direct measurements of pulsed-structure and turbulence of turbidity currents overspilling from a submarine channel. *Geophysical Research Letters*, *53*, e2025GL121222. https://doi.org/10.1029/2025GL121222

Received 13 DEC 2025
Accepted 7 FEB 2026

**Abstract** Turbidity currents transport vast amounts of sediment, carbon, and heat along submarine channels, yet their overspill onto channel-levees and abyssal mixing remain poorly constrained due to lack of direct observations. Ocean-bottom seismometers (OBS) deployed on the Congo Canyon–Channel levees captured the structure and turbulence of overspill during an exceptionally large canyon-flushing event in 2020. Overspill persisted for 3 weeks and comprised numerous short (20-min to 2-hr) pulses focused at outer bends. Spectra during overspill show well-resolved turbulence inertial subranges, yielding event-average dissipation rates of $10^{-6}$–$10^{-5}$ $m^2$ $s^{-3}$, comparable to energetic internal-tide breaking. Abyssal overspill can therefore be long-lasting and highly pulsed, providing an episodic but locally important source of deep-ocean mixing. This new view of levee overspill has important implications for building levees and the interpretation of ancient turbidites. Individual levee deposits may be formed incrementally by many pulses of dilute and fine-grained flow from a single turbidity current.

**Plain Language Summary** Turbidity currents are seabed avalanches that transport sediment, carbon, and heat from the continental margins into the deep ocean. As these currents move through submarine channels, part of the sediment-rich flow can spill over the channel margins onto the surrounding levees. This "overspill" builds channel-levee complexes, which are a key building block of submarine fans, the largest sedimentary bodies on Earth. Overspill may also influence turbulent mixing and ventilation near submarine channels, but how turbidity currents spill onto levees and interact with abyssal waters remains poorly constrained due to the lack of direct observations. Here we show that overspill can be monitored using ocean-bottom geophones and hydrophones on channel levees, which recorded subtle vibrations and acoustic signals as sediment-laden overspill passed over them. Using this approach, we captured overspill during an exceptionally large turbidity current in 2020 in the Congo Channel, and documented its structure and turbulence intensity. Overspill persisted for 3 weeks and comprised many short, repeated pulses that generated extremely strong turbulence, among the highest levels recorded at >4 km depth. This prolonged overspill behavior provides an important yet previously overlooked source of deep-ocean mixing, and helps explain how levees grow and how ancient turbidites are built.

## 1. Introduction

Turbidity currents are sediment-laden flows that can travel hundreds to thousands of kilometers across the ocean floor, and whose upper parts are highly turbulent (Heezen & Ewing, 1952; Talling et al., 2022, 2023). These flows carve submarine channels with upraised levees that route globally significant volumes of sediment, carbon, and nutrients to the deep-sea (Canals et al., 2006; Galy et al., 2007; Kao et al., 2010; Shepard, 1972). These channel-levee complexes form the building blocks of submarine fans, which include the largest sedimentary bodies on Earth, and are important archives of its history (Bouma et al., 1985). Transport of sediment and carbon to the deep-sea by turbidity currents depends critically on overspill from submarine channels onto adjacent levees. Overspill profoundly affects how flows lose momentum and sediment, and how flows mix with surrounding ocean water.

However, overspill remains poorly constrained due to the lack of direct observations, leaving key process–product linkages unresolved. Classical models describe overspill as a dilute, spatially decelerating (waning) flow that steadily loses energy. Such waning flows are inferred to produce deposits (turbidites) that thin and fine-

upwards and away from the channel, which typically comprise laminated silts capped by mud (Hansen et al., 2015; Hiscott et al., 1997; Peakall et al., 2000; Piper, 1978; Talling et al., 2012). Such thin, fine-grained turbidites are ubiquitous in levee sequences, and their study underpins knowledge of turbidity-current dynamics, submarine fan construction, and frequency and triggers of flows over geological time scales (Peakall et al., 2000; Piper, 1978; Stow & Bowen, 1980). Interpreting levee deposits must be based on understanding of overspill processes, including where and when overspill initiates, the overall duration and internal velocity-structure of overspill, and its turbulence structure.

It is also poorly understood how overspilling turbidity currents affect turbulent mixing in the deep-sea. Long-term variation of deep-ocean turbulence is commonly inferred from moored temperature sensors, which use small-scale thermal fluctuations and the temperature–density relationship to estimate turbulent dissipation rates, denoted by $\varepsilon$ (Thorpe, 1977). Internal-wave breaking above rough topography is widely regarded as the dominant source of abyssal mixing, producing long-term $\varepsilon$ levels of order $10^{-7}$ $m^2$ $s^{-3}$ in topographically rough regions (van Haren et al., 2016; van Haren & Gostiaux, 2012), whereas background abyssal-interior values are typically of order $10^{-11}$–$10^{-10}$ $m^2$ $s^{-3}$ (Yasuda et al., 2021). In contrast, turbulence produced by overspilling turbidity currents has not yet been directly quantified because such events are brief, hazardous, and rarely observed by traditional approaches.

Here we present direct observations of submarine channel overspill, recorded in the Congo Canyon–Channel during an exceptionally powerful canyon-flushing turbidity current in January–February 2020. This event broke multiple seabed cables, traveled >1,100 km to the deep-sea (Talling et al., 2022), and together with a second major March 2020 flow eroded and transported 43 ± 15 Mt of terrestrial organic carbon (Baker, Hage, et al., 2024). This mass is comparable to the estimated global annual burial of terrestrial organic carbon in marine sediments (40–80 Mt $yr^{-1}$; Hilton & West, 2020). Strategically sited ocean-bottom seismometers (OBS) on the channel levees recorded seismic and hydroacoustic signals of the January-February and March 2020 canyon-flushing flows (Baker, Hage, et al., 2024; Kunath, Talling, Lange, et al., 2025). These records include passage of the main channelized flow, but also signals at certain OBS that we interpret as overspill from the channel engulfing the OBS. This interpretation is supported by a sustained bottom-water temperature increase at one OBS after the channelized front had passed (Baker, Talling, Burnett, et al., 2024), and by previous reports of OBS engulfment by energetic near-bed flows producing similar seismic signatures (Corela et al., 2022). These unique OBS records reveal the duration, temporal structure, and turbulence of overspill, providing new insight into levee construction and how sediment, organic carbon, and heat are redistributed in the deep-sea.

Our overall aim is to show how OBSs can directly monitor turbidity current overspill and turbulence. Specifically, we seek to understand (a) the timing, duration, and spatial variability of overspill across multiple sites, (b) quantify turbulence dissipation rates within overspill, and place them in the context of deep-ocean mixing budgets, (c) evaluate the spatiotemporal controls that initiate overspill pulses, and (d) assess implications for levee-deposit architecture and for interpreting turbidite sequences.

## 2. Turbidity Currents in the Congo Canyon and Channel

The Congo Canyon incises into the shelf over its first ~150 km, where it has vertical relief of up to 1,200 m (Figure 1a). The canyon then evolves into a less deeply (100–250 m) incised submarine channel with depositional flanking-levees, which extends more than 1,100 km to the abyssal plain (Babonneau et al., 2002; Figure 1b). The head of the canyon lies within the estuary of the Congo River, which has the second largest water discharge and fifth largest particulate organic carbon flux of any river on Earth (Milliman & Farnsworth, 2013). The upper part of the Congo Submarine Canyon experiences turbidity currents that typically last for 5–10 days, with flows occurring for ~20–40% of the total time at water depth of ~1,750 m (Azpiroz-Zabala et al., 2017; Simmons et al., 2020; Talling et al., 2022). Most flows terminate within the upper canyon, but less frequent and more powerful flows flush sediment through the canyon-channel and into the deep sea (Kunath, Talling, Lange, et al., 2025; Talling et al., 2022).

From October 2019 to May 2020, 10 OBSs (OBS1–OBS10) were deployed on terraces and levees 0.5–3.0 km from the axis of the Congo Canyon–Channel (Figure 1) (Baker, Talling, Burnett, et al., 2024; Kunath, Talling, Lange, et al., 2025). These instruments were complemented by moorings equipped with Acoustic Doppler Current Profilers (ADCPs) on the canyon–channel floor (Talling et al., 2022). Seismic records from OBS sites were compared to ADCP-derived velocities from adjacent moorings, at least for relatively slow (<2–3 m $s^{-1}$)

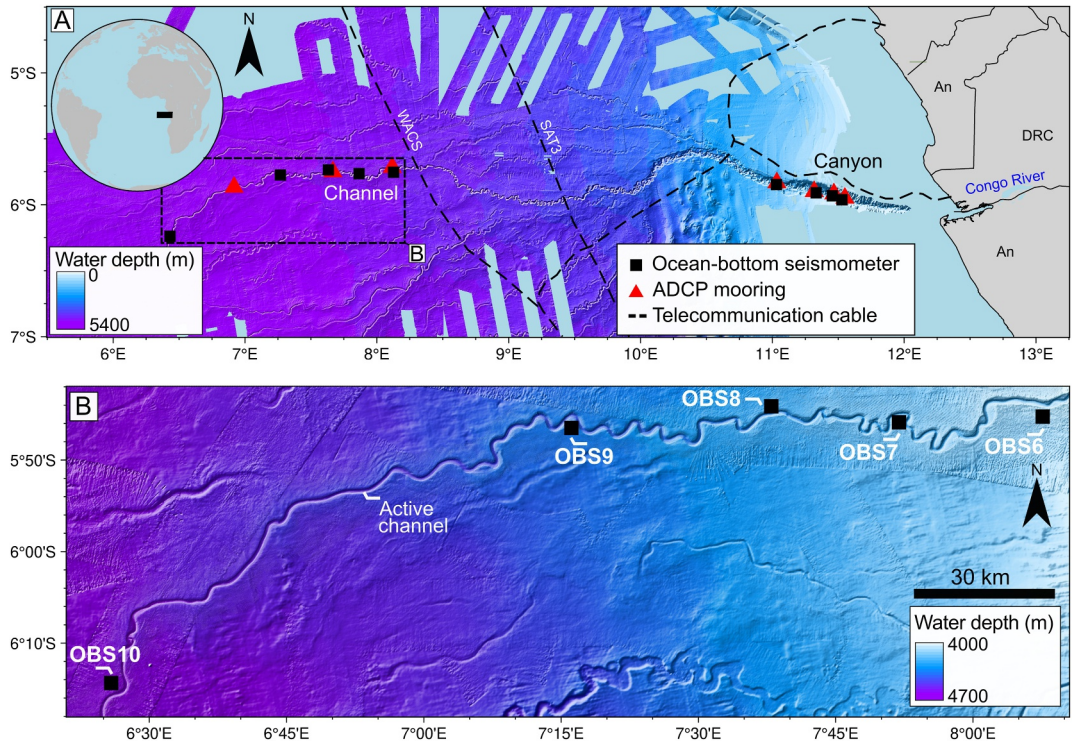


**Figure 1.** Bathymetric maps of study area and instrument locations. (a) The Congo Canyon-Channel system, located offshore West Africa (location in inset), showing the placement of instruments. Acoustic Doppler Current Profiler (ADCP) moorings (red triangles) were located in the channel axis, where they were eventually broken by powerful turbidity currents (together with the South Atlantic 3 (SAT-3) and West Africa Cable System telecommunication cables), whilst the Ocean Bottom Seismometers (OBSs; black squares) were located on the canyon terraces and channel levees, out of harm's way. An, Angola; DRC, Democratic Republic of the Congo. (b) Bathymetric map of the channel (rectangle in a) showing the locations of OBS6 to OBS10.

turbidity currents that did not break the ADCP mooring-lines. This comparison shows that the OBSs primarily record the fast-moving (>1.5 m $s^{-1}$) dense zone at the front of channelized flows, rather than their more dilute trailing body (Baker, Talling, Burnett, et al., 2024).

In contrast to these slower flows, an unusually powerful canyon-flushing turbidity current on 14–16 January 2020 broke all ADCP mooring-lines, which was preconditioned by a major Congo River flood with an estimated recurrence interval of 20–50 years (Talling et al., 2022). This is the event whose overspill we analyze here, based on records from OBS located on the channel levees (OBS6-10; Figure 1b). Transit speeds inferred from cable-breaks, ADCPs, and OBSs show that flow fronts traveled at 5–8 m $s^{-1}$ over >1,100 km (Baker, Talling, Burnett, et al., 2024; Kunath, Talling, Lange, et al., 2025; Talling et al., 2022), making it the longest-runout sediment flows yet measured in action on Earth (Talling et al., 2022).

## 3. Materials and Methods

We analyzed three-component geophone and hydrophone data from OBS6–OBS10, located 1.5–2.9 km from the Congo Channel axis on overbank levees (Figures S1–S5 in Supporting Information S1). Seismic waveforms were corrected for instrument response, band-pass filtered, response corrected to ground velocity, and combined across the three components (E–W, N–S, vertical) to calculate kinetic-energy time series $E_k = \frac{1}{2}(v_x^2 + v_y^2 + v_z^2)$ (Supporting Information S1).

Spectrograms were computed from $E_k$ and hydrophone records, and overspill was identified by analyzing the spectra together with a band-limited (≤30 Hz) $E_k$ maximum-power time series. Overspill pulses were defined where spectral power exceeded both the station-specific noise floor and a prominence threshold of ≥7 dB above adjacent background levels, allowing us to quantify the duration and pulsed structure of the overspill.

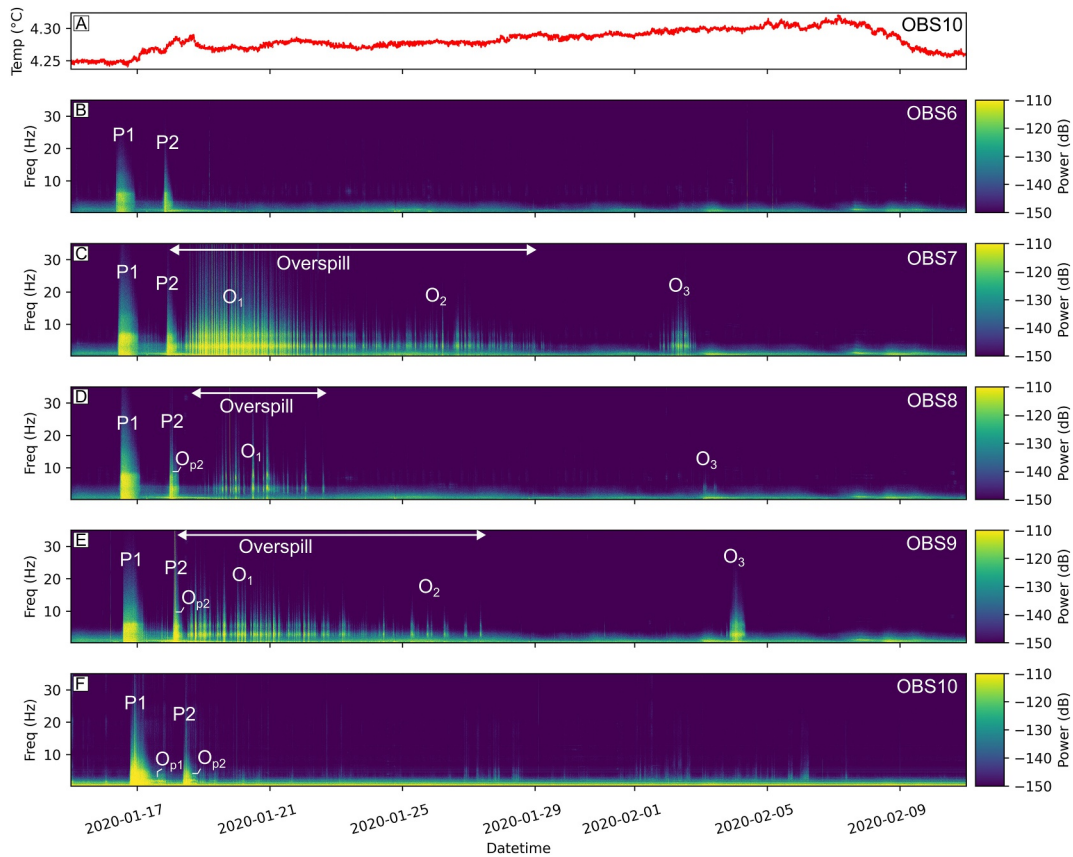


**Figure 2.** Signatures of the Congo Canyon-flushing turbidity current. (a) Near-seafloor temperature time-series recorded at OBS10. (b)–(f) Spectrograms of seismic kinetic energy ($E_k$) from ocean-bottom seismometers (OBS)s deployed on levees outside the Congo Channel, ordered by increasing distance from the river mouth (see Figure 1 for OBS locations). Seismic power is shown in units of dB re ($m^2$ $s^{-2}$)/Hz. The channelized turbidity current produces two initial pulses (P1 and P2) associated with the fast-moving, dense frontal parts (Baker, Talling, Burnett, et al., 2024; Kunath, Talling, Lange, et al., 2025) of channel-confined flow. At OBS7–OBS10, elevated $E_k$ persists for ∼3 weeks, documenting repeated phases of overspill from the channel onto the levee that engulf the OBS. These periods of overspill include those from frontal parts of the flow ($O_{p1}$ and $O_{p2}$) coinciding with in-channel pulses P1 and P1, as well as more prolonged overspill ($O_1$–$O_3$) from the trailing body and tail of the turbidity current.

Turbulence within these pulses was identified from its canonical spectral structure: a well-resolved power-law with exponent $p$ of −5/3 in the inertial subrange of turbulence, followed by a roll-off to steeper slopes ($p < \sim -4$ to $-5$) marking the onset of viscous dissipation (Tennekes & Lumley, 1972; Warhaft, 2000). Turbulence dissipation rates ($\varepsilon$) were then estimated from the transition frequency between the inertial and viscous subranges using Kolmogorov scaling (Pope, 2000). Full processing details, parameter choices, and sensitivity tests are provided in Supporting Information S1.

## 4. Results and Discussion

### 4.1. Seismic, Acoustic and Thermal Footprint of Overspill

We identify levee overspill using its characteristic seismic, acoustic, and thermal signatures.

Spectrograms from OBS geophones have previously been used to characterize the signal strength, dominant frequencies, and duration of the within-channel component of Congo Canyon turbidity currents (Kunath, Talling, Lange, et al., 2025). These appeared as high-amplitude pulses reaching ∼–80 dB, with most energy below 10 Hz and amplitudes ∼30 dB above ambient noise (Figures 2b–2f). For the canyon-flushing flow analyzed here, frontal-head pulses (P1 and P2 in Figure 2) showed emergent onsets, delayed peaks, and long decays back to background levels, and they persisted for 5–14 hr (Baker, Talling, Burnett, et al., 2024). These characteristics

reflect seismic attenuation as the flow approaches and passes each OBS, and temporal changes in surge dynamics within the fast-moving frontal head (Kunath, Talling, Lange, et al., 2025).

Here we show that overspill pulses also appeared as high-amplitude signals with levels up to about −80 dB and dominant energy below 10 Hz (Figures 2b–2f). Unlike the confined axial flows, these overspill pulses began abruptly (Figures S6–S8 in Supporting Information S1). This is consistent with generation by a local overspill source on the levee that suddenly engulfs and vibrates the OBS, rather than the axial turbidity current gradually approaching the OBS location, which would produce more gradual, emergent onsets. At OBS10, these impulsive onsets for overspilling flow were followed by hours-long, narrow-band harmonics below 8 Hz (Figure S9 in Supporting Information S1). Such response is characteristic of this OBS type when it is engulfed within a flow, as the frame and appendages resonate in local turbulence (Corela et al., 2022).

Hydrophones mounted on the OBSs did not clearly record the within-channel arrivals of these turbidity currents documented by OBS geophones (Baker, Talling, Burnett, et al., 2024). In contrast, both hydrophone and geophones clearly captured overspill pulses outside the channel (Figures S6–S8a, and S8b in Supporting Information S1). Their spectra exhibit identical shapes and strong spectral coherence below ∼10 Hz (Figures S6–S8c in Supporting Information S1), indicating a strong frequency-dependent correlation of the time-varying signals and demonstrating that geophones and hydrophones responded to the same local process within this frequency band.

The overspill spectra exhibit a spectral gradient of $p = -5/3$, associated with the inertial subrange of turbulence, and a common roll-off to $p < -5$ at higher frequencies in both geophone and hydrophone records (Figures 3a and 3b; Figure S10 in Supporting Information S1). This spectral match across the two sensor types suggests a common locally-sourced, turbulence-generated pressure fluctuations near the seabed, as overspilling flow passes the station. Hydrophones record these pressure fluctuations directly, whereas geophones sense them indirectly through vibration or rocking of the OBS frame on compliant sediment. During quiet intervals between pulses, no turbulence inertial subrange was resolved (Figures 3c and 3d).

Overspill signals were accentuated at sharp outer bends (OBS7–OBS9) and absent along straighter reaches of the channel (OBS6; Figure 2). This spatial pattern supports our overspill interpretation, as curvature focuses and accelerates the upper part of the flow toward the outer bend, promoting spillover and forming outer-levee sediment waves observed in the Congo system and many other submarine channels (Gervais et al., 2001; McHugh & Ryan, 2000).

Independent bottom-water temperature at OBS10 showed a sustained anomaly coincident with the turbidity current and its subsequent pulses (Figure 2a), confirming that the station was inundated by a relatively warm layer of the flow during the overspill interval, and no comparable temperature anomalies occurred elsewhere in the 10-month deployment (Figure S11 in Supporting Information S1).

Alternative explanations for the origin of these signals such as earthquakes, storms, tides, internal waves, marine mammals or ship noise are inconsistent with these observations. Such sources would produce basin-wide, coherent arrivals with clear far-field precursors, or would not be spatially focused at sharp outer bends, or coincide with ∼3-week-long canyon-flushing turbidity currents and associated bottom-temperature anomalies, and they would not generate matched geophone–hydrophone inertial-subrange spectra with a common dissipation-range roll-off that record local turbulence at the levee crest.

### 4.2. Structure of Overspill

Channel-levee overspill occurred intermittently over 3 weeks between 17 January and 4 February 2020, with site-specific onsets. At OBS7–OBS9 it began ∼2 hr into Pulse 2 (P2) and was absent in the first frontal head pulse (P1) (Figure 2, Figures S6–S8 in Supporting Information S1). This indicates that P1 was thinner than the levee crest heights, which are ∼175, ∼150, and ∼125 m (Figures S2–S4 in Supporting Information S1). At distal OBS10, overspill signatures appeared during both P1 and P2 (Figure S9 in Supporting Information S1), consistent with a shallower levee-crest of ∼75–80 m that allowed both pulses of the high-momentum head (P1 and P2) to intermittently exceed the levee crest height at this location.

Seismic records of overspilling flow show a repeatable sequence, here termed overspill phases O1–O3: an early clustered burst that intensified over 1–2 days (O1), a several-day taper into ∼1 week of intermittent pulses (O2), a multi-day quiescent gap, and a ∼1-day renewal (O3; Figures 2c–2e). Individual pulses were short (≤2.5 hr), and

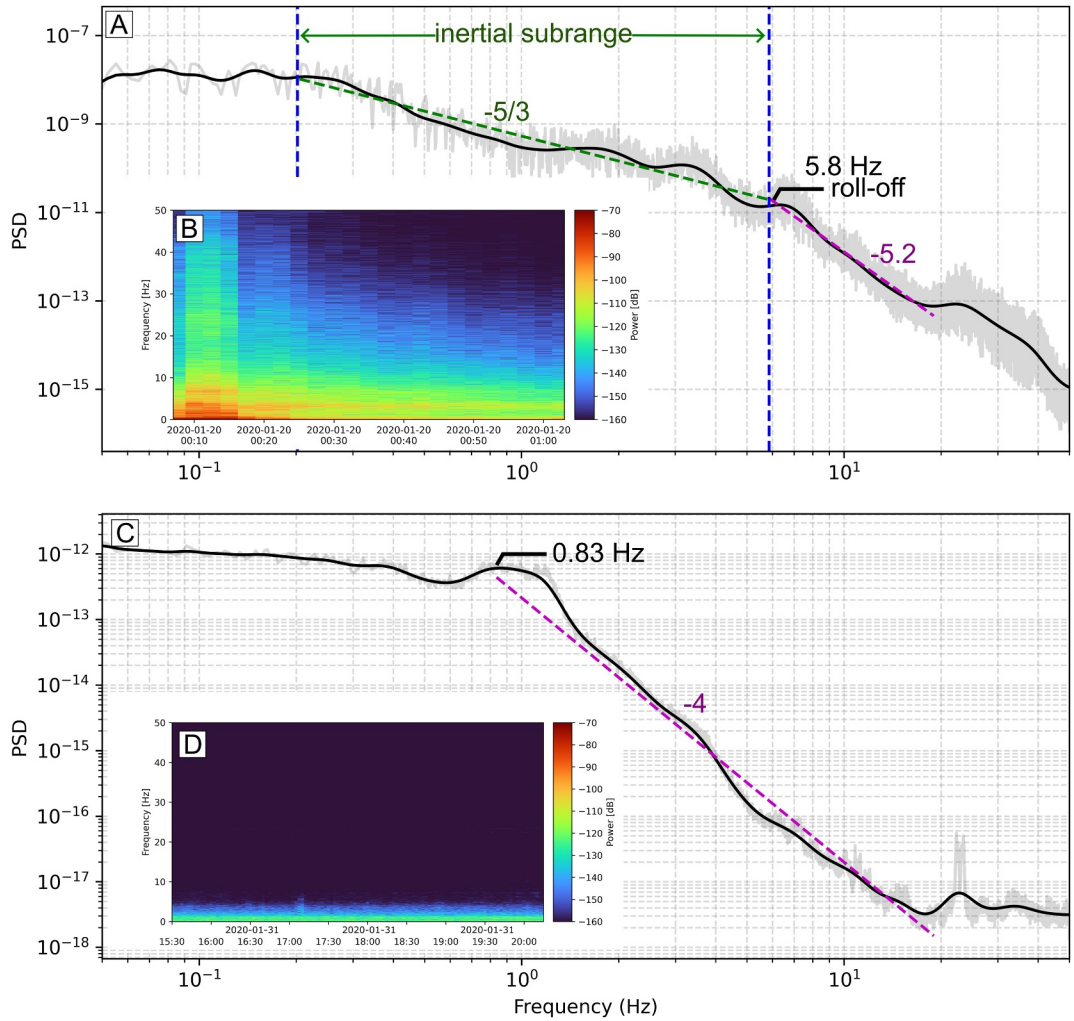


**Figure 3.** (a) Seismic kinetic energy ($E_k$) power spectral density (PSD) at OBS7 computed over a one-hour interval of overspilling turbidity current on 20 January at 00:07 UTC. The spectrum has a gradient ($p$) of −5/3 power law between frequencies of 0.2 and 5.85 Hz (inertial subrange of turbulence) before steepening to a gradient ($p$) of −5.2 in the turbulent dissipation range. The dissipation-range roll-off frequency (5.8 Hz) implies a turbulent kinetic energy dissipation rate of $\varepsilon \approx 4.5 \times 10^{-5}$ to $1.2 \times 10^{-4}$ m$^2$ s$^{-3}$, depending on the assumed relationship between roll-off frequency and dissipation (see Supplementary Information S1). (b) Corresponding 1-hr $E_k$ spectrogram from the overspill interval. (c) $E_k$ PSD from a quiescent interval with no turbidity current at OBS7 (corresponding $E_k$ spectrogram in d), showing no $p = -5/3$ inertial subrange. Note the different $y$-axis range in (c) relative to (a).

frequently multi-peaked with 20–60 min spacing, especially during O1–O2 (Figures S12 and 14c–14e in Supporting Information S1).

At OBS7, $E_k$ power rose from ∼–120 to ∼–80 dB during O1, then decreased toward ∼–100 dB over ∼3.5 days while remaining above ambient; O2 showed similar levels but with near-ambient intervals between pulses, and O3 renewed activity to O2-like or higher power (Figure 2e; Figures S11a and S11b in Supporting Information S1). Although power generally decreases from O1 to O3, the evolution is non-monotonic and intermittently re-energized.

The active fraction ($f_{active}$), defined as the proportion of the O1–O3 window occupied by overspill pulses, was 0.64 at OBS7, 0.41 at OBS9, and 0.16 at OBS8. At OBS10, distinctive pulses were confined to ∼1–2 day after P2 ($f_{active}$ ∼0.05–0.1), yet bottom-water temperature stayed elevated for ∼20 days and even continued to rise after P2 until a sharp drop near day 20 (Figure 2a). Because turbulent mixing is irreversible and a return to background requires advective replacement, this prolonged temperature rise is compatible with either continuous overspill

that maintains near-bed mixing or repeated pulse trains whose cumulated effects are recorded in the temperature signal, even when individual seismic pulses are no longer clearly resolved at this site.

### 4.3. Down-Canyon Evolution

To assess how overspill evolves downstream, we examine changes in the timing and duration of pulses at successive OBS sites. The O3 pulse occurs only at OBS7–OBS9 and follows a several-day quiet period, implying that it originated from the same trailing channelized body segment migrating down-channel. This arrival pattern yields a trailing-body transit speed of about 0.55 m $s^{-1}$ between stations, well below frontal-head velocities of 4.6–7.2 m $s^{-1}$ in this turbidity current (Baker, Talling, Burnett, et al., 2024) and comparable to trailing-body speeds of about 0.8 m $s^{-1}$ reported for smaller Congo Canyon events in shallower water (<2 km) (Simmons et al., 2020).

The evolving footprint of O3 is mirrored by changes in overspill duration. Overspill lasts about 16 days at OBS7, about 18 days at OBS9, and ∼21 days at OBS10, as inferred from the bottom-temperature anomalies ∼230 km farther downstream from OBS7 (Figure 2a). This progressive lengthening of O3 indicates that the trailing body stretched along the channel as the fast, dense frontal head outpaced a slower body that incorporated eroded sediment backward, thereby maintaining the observed near-steady frontal speeds (Baker, Talling, Burnett, et al., 2024).

### 4.4. Turbulence Dissipation Rates and Mixing Budgets

During representative 30–60-min pulses, mean $\varepsilon$ values range from $2.5 \times 10^{-5}$ to $4.5 \times 10^{-5}$ $m^2$ $s^{-3}$ (or $6.75 \times 10^{-5}$ to $1.2 \times 10^{-4}$ $m^2$ $s^{-3}$), depending on the assumed relationship between roll-off frequency and dissipation (Supporting Information S1). Intervals without distinctive pulses lack a resolved inertial subrange and dissipation-range roll-off, which indicates a shift toward weakly turbulent conditions.

These pulse values far exceed background turbulence dissipation rates in abyssal-plains, which are typically of order $10^{-10}$ $m^2$ $s^{-3}$, and open-ocean interior values of order $10^{-11}$ $m^2$ $s^{-3}$ (Yasuda et al., 2021), by approximately six orders of magnitude. For comparison, $\varepsilon$ values of order $10^{-5}$ $m^2$ $s^{-3}$ have previously been reported only during short periods of extreme internal-tide breaking above steep topography. An upslope-propagating bore over an underwater seamount produced peak $\varepsilon$ of order $10^{-5}$ $m^2$ $s^{-3}$ during about 10 min, supplying ∼60% of the turbulence over a tidal cycle, where mean dissipation rates were of order $10^{-7}$ $m^2$ $s^{-3}$ (van Haren & Gostiaux, 2012). For internal tides breaking above the steep slope of Mount Josephine in the NE Atlantic, 4-day depth-averaged $\varepsilon$ were 1.3 (±1.0) $\times 10^{-7}$ $m^2$ $s^{-3}$ during neap tide and 6 (±4) $\times 10^{-7}$ $m^2$ $s^{-3}$ during spring tide (van Haren et al., 2016).

We also estimated the event-scale dissipation rate $\varepsilon_{3wk}$ over the 3-week overspill interval. Using $f_{active}$ of overspill pulses (Supporting Information S1), $\varepsilon_{3wk}$ lies in the range (1.3–2.3) $\times 10^{-6}$ to (1.6–2.9) $\times 10^{-5}$ $m^2$ $s^{-3}$. These values remain well above typical abyssal-plain and open-ocean interior levels and are comparable to those from energetic internal-tide breaking. The exceptionally high $\varepsilon_{3wk}$ values indicate that overspill provides short-lived but extremely energetic mixing above the channel-levee flanks, despite the stations having been positioned >1–2 km from the thalweg, where rapid decay of turbulence might otherwise be expected.

If comparable canyon-flushing overspill recurs every 20–50 years, a similar recurrence rate to major Congo River floods that prime such events (Talling et al., 2022), then the implied long-term local mixing contribution along the near-channel abyssal plain is of order $10^{-8}$ $m^2$ $s^{-3}$. Infrequent overspill from canyon-flushing turbidity currents injects strong turbulence into the deep ocean over multiweek timescales, and it may influence stratification, ventilation, and sediment–water exchange near active submarine channels and fan systems over years to decades. These values quantify an episodic mixing pathway that is absent from current abyssal budgets.

### 4.5. How Do Overspill Pulses Originate?

Overspill exhibits pulsing across multiple timescales, with individual pulses lasting minutes to a few hours, with individual pulses grouped into day-scale clusters (O1–O3; Figure 2). This multiscale variability implies that several processes modulate the thickness and momentum of overspilling flow across the channel margins. Although our data cannot uniquely resolve how pulses originate, prior observations of Congo Canyon turbidity currents point to three non-exclusive potential mechanisms for generating pulses.

First, in the upper Congo Canyon, long-duration pulses (2–6 hr) have been observed and are thought to originate from multiple upstream events at the river mouth, preconditioned by major Congo River floods and subsequently triggered by spring tides (Baker, Talling, Burnett, et al., 2024; Talling et al., 2022). These pulses traveled at different speeds and amalgamated before reaching the deeper channel sites that we study here (Baker, Talling, Burnett, et al., 2024). External processes can also create shorter minute- to hour-scale pulses, for example, through localized erosion and entrainment of seabed sediment that form denser, faster packets within the flow (Kunath, Talling, Lange, et al., 2025). A retrogressive canyon-wall failure triggered by the same event analyzed here supplied 10–30-min sediment pulses into the trailing body rather than the frontal head (Kunath, Talling, Urlaub, et al., 2025), illustrating this pathway.

Second, internal instabilities can spontaneously amplify small perturbations into shorter pulses, analogous to roll-waves in subaerial events, including debris flows (Zanuttigh & Lamberti, 2007). Such instabilities have also been documented within the dense, fast frontal head of this canyon-flushing event (Kunath, Talling, Lange, et al., 2025), producing 5–30-min pulses. These durations fall within, or form the short-period end of, the 20–120-min overspill pulses documented here. Thus, part of the minute-scale variability recorded at the levee may originate from internally driven instabilities of channelized sediment flow rather than solely from external source forcing or slope failures. These internal instabilities may also propagate into the trailing body, or be inherited from surges shed from the head, and thereby become superimposed on the longer-term variability imposed by external river-mouth sediment inputs and canyon-wall failures.

Third, tidal modulation imposes a semidiurnal rhythm. Power spectral density estimates exhibit a semidiurnal M2 band across stations (Figure S15 in Supporting Information S1). Internal tides can propagate up and down the canyon at speeds of order 0.1 m $s^{-1}$ and may alternately oppose or enhance overspill by modulating near-bed velocity, mixing, and layer thickness, providing a plausible mechanism for the observed tidal-scale variability. Prior observations identified tidal influences on the internal structure of smaller Congo Canyon turbidity currents at ~2,000 m water depth (Simmons et al., 2020); our observations suggest that similar processes also affect levee overspill at abyssal depths.

Across these mechanisms and timescales, surges that travel at different speeds can merge, intermittently thicken the channelized body, and locally enhance near-crest momentum, thereby promoting overspill. Some surges generated in the frontal head are likely incorporated into the trailing body, leaving remnant thickness and velocity anomalies that continue to drive overspill downstream. The strongest expression of overspill is expected at sharp outer bends, where curvature elevates the flow toward the outer levee.

### 4.6. Process-to-Product Inference

Previously it was assumed that overspilling flows would comprise single pulses, whose strength waned over time and decreased with distance from the channel crest (Hansen et al., 2015; Piper, 1978; Stow & Bowen, 1980), leading to deposits that fined upwards and laterally. Our observations reveal that overspill can rather behave as a highly-pulsed and intermittently active process, in which turbulence is repeatedly regenerated. The strongly pulsed nature of overspill will also affect sediment transport onto levees, and associated levee deposits.

Individual deposits (beds) described from levee settings typically display a single overall fining-upward trend, often with a silty or sandy base with ripples (Bouma $T_C$ or $T_D$ divisions), overlain by an interval of finer mud (Bouma $T_E$ division), whilst in other cases these thin beds comprise only turbidite mud (Hansen et al., 2015; Hiscott et al., 1997; Peakall et al., 2000; Piper, 1978; Talling et al., 2012). Levee deposit that show inverse grading or more complex grading patterns have been observed (Hansen et al., 2015; Hiscott et al., 1997), but individual beds with numerous pulses of coarser and finer grains are not commonly described in levee sequences. To explain this paucity, we propose that the overspilling flows tend to be dilute and fine-grained, and that they may produce complex patterns of grain size in fine-grained muddy ($T_E$) deposits, but those subtle variations in grain size are too small to observe visually within thin muddy turbidites. There are very few detailed grain size analyses of the muddy ($T_E$) intervals in levee turbidites (e.g., Hiscott et al., 1997), and their resolution may also be insufficient to document subtle fluctuations in muddy grain-sizes in such beds. Grain size fluctuations may occur vertically over a few millimeters, ensuring that exceptionally fine sample spacing would also be needed.

It has also been proposed that pulsed turbidites comprising multiple fining upward sequences are strongly diagnostic of turbidity currents triggered by earthquakes (Goldfinger et al., 2012; Nakajima & Kanai, 2000), and

this assumption can have important implications for deriving reliable records of major earthquakes from turbidites. Here we show that pulsing can also originate via other processes for overspilling flows, without the occurrence of an earthquake. Thus, caution is needed when inferring an earthquake trigger from pulsed grading patterns.

Our observations therefore show that overspill of large turbidity currents can be highly pulsed, rather than comprising a single episode of temporally and spatially decelerating flow (Peakall et al., 2000). We also show that overspill from large canyon flushing turbidity currents can be sustained for several weeks. Overspill repeatedly renews shear and turbulence along the channel flanks and provides a previously unaccounted source of abyssal mixing and ventilation near active submarine channels. Finally, our study illustrates that OBS arrays can resolve turbulence within deep-sea sediment, offering a practical means to monitor mixing, sediment export, and geohazards along submarine channel systems.

## Conflict of Interest

The authors declare no conflicts of interest relevant to this study.

## Data Availability Statement

The raw OBS data (Baker, Talling, Peirce, et al., 2024) used to record turbidity currents in this study are available at the British Oceanographic Data Centre (BODC) with no access conditions.

**Acknowledgments**
We gratefully acknowledge the shipboard parties of the RRS James Cook cruises JC187 and JC209. Our thanks to GEOMAR's and NERC's Ocean Bottom Instrumentation Facility for providing OBSs. Open Access funding enabled and organized by Projekt DEAL.

## References

Azpiroz-Zabala, M., Cartigny, M. J., Talling, P. J., Parsons, D. R., Sumner, E. J., Clare, M. A., et al. (2017). Newly recognized turbidity current structure can explain prolonged flushing of submarine canyons. *Science Advances*, *3*(10), e1700200. https://doi.org/10.1126/sciadv.1700200

Babonneau, N., Savoye, B., Cremer, M., & Klein, B. (2002). Morphology and architecture of the present canyon and channel system of the Zaire deep-sea fan. *Marine and Petroleum Geology*, *19*(4), 445–467. https://doi.org/10.1016/s0264-8172(02)00009-0

Baker, M. L., Hage, S., Talling, P. J., Acikalin, S., Hilton, R. G., Haghipour, N., et al. (2024). Globally significant mass of terrestrial organic carbon efficiently transported by canyon-flushing turbidity currents. *Geology*, *52*(8), 631–636. https://doi.org/10.1130/g51976.1

Baker, M. L., Talling, P. J., Burnett, R., Pope, E. L., Ruffell, S. C., Urlaub, M., et al. (2024). Seabed seismographs reveal duration and structure of longest runout sediment flows on Earth. *Geophysical Research Letters*, *51*(23), e2024GL111078. https://doi.org/10.1029/2024gl111078

Baker, M. L., Talling, P. J., Peirce, C., & Pitcairn, B. (2024). Ocean bottom seismograph data deployed along the Congo Submarine Canyon and Channel (Atlantic Ocean) on cruise JC187, September 2019-September 2020. (Version 1) [Dataset]. *NERC EDS British Oceanographic Data Centre NOC*. https://doi.org/10.5285/1D4A3BF0-FEAB-465C-E063-7086ABC0EF74

Bouma, A. H., Normark, W. R., & Barnes, N. E. (1985). *Submarine fans and related turbidite systems*. Springer.

Canals, M., Puig, P., de Madron, X. D., Heussner, S., Palanques, A., & Fabres, J. (2006). Flushing submarine canyons. *Nature*, *444*(7117), 354–357. https://doi.org/10.1038/nature05271

Corela, C., Loureiro, A., Duarte, J. L., Matias, L., Rebelo, T., & Bartolomeu, T. (2022). The OBS noise due to deep ocean currents. *Natural Hazards and Earth System Sciences Discussions*, *2022*, 1–21.

Galy, V., France-Lanord, C., Beyssac, O., Faure, P., Kudrass, H., & Palhol, F. (2007). Efficient organic carbon burial in the Bengal fan sustained by the Himalayan erosional system. *Nature*, *450*(7168), 407–410. https://doi.org/10.1038/nature06273

Gervais, A., Mulder, T., Savoye, B., Migeon, S., & Cremer, M. (2001). Recent processes of levee formation on the Zaire deep-sea fan. *Comptes Rendus de l'Academie des Sciences - Series IIA: Earth and Planetary Science*, *332*(6), 371–378. https://doi.org/10.1016/s1251-8050(01)01550-6

Goldfinger, C., Nelson, C. H., Morey, A. E., Johnson, J. R., Patton, J., Karabanov, E., et al. (2012). *Turbidite event History—Methods and implications for Holocene paleoseismicity of the cascadia subduction Zone professional paper 1661–F*. USGS. https://doi.org/10.3133/pp1661F

Hansen, L. A., Callow, R. H., Kane, I. A., Gamberi, F., Rovere, M., Cronin, B. T., & Kneller, B. C. (2015). Genesis and character of thin-bedded turbidites associated with submarine channels. *Marine and Petroleum Geology*, *67*, 852–879. https://doi.org/10.1016/j.marpetgeo.2015.06.007

Heezen, B. C., & Ewing, M. (1952). Turbidity currents and submarine slumps, and the 1929 Grand Banks earthquake. *American Journal of Science*, *250*(12), 849–873. https://doi.org/10.2475/ajs.250.12.849

Hilton, R. G., & West, A. J. (2020). Mountains, erosion and the carbon cycle. *Nature Reviews Earth & Environment*, *1*(6), 284–299. https://doi.org/10.1038/s43017-020-0058-6

Hiscott, R. N., Hall, F. R., & Pirmez, C. (1997). Turbidity-current overspill from the Amazon channel: Texture of the silt/sand load, paleoflow from anisotropy of magnetic susceptibility, and implications for flow processes. In *Proceedings-ocean drilling program scientific results* (pp. 53–78). National Science Foundation.

Kao, S. J., Dai, M., Selvaraj, K., Zhai, W., Cai, P., Chen, S. N., et al. (2010). Cyclone-driven Deep sea injection of freshwater and heat by hyperpycnal flow in the subtropics. *Geophysical Research Letters*, *37*(21), 1–5. https://doi.org/10.1029/2010GL044893

Kunath, P., Talling, P. J., Lange, D., Chi, W. C., Baker, M. L., Urlaub, M., & Berndt, C. (2025). Ocean-bottom seismometers reveal surge dynamics in Earth's longest-runout sediment flows. *Communications Earth & Environment*, *6*(1), 147. https://doi.org/10.1038/s43247-025-02137-z

Kunath, P., Talling, P. J., Urlaub, M., Berndt, C., Chi, W. C., & Baker, M. (2025). Ocean-bottom seismometers document how submarine landslides develop and grow. *Communications Earth & Environment*, *6*(1), 871. https://doi.org/10.1038/s43247-025-02918-6

McHugh, C. M. G., & Ryan, W. B. F. (2000). Sedimentary features associated with channel overbank flow: Example from the Monterey Fan. *Marine Geology*, *163*(1–4), 199–215. https://doi.org/10.1016/s0025-3227(99)00098-5

Milliman, J. D., & Farnsworth, K. L. (2013). *River discharge to the coastal Ocean: A global synthesis*. Cambridge Univ. Press.
Nakajima, S., & Kanai, K. (2000). Sedimentary features of seismoturbidites triggered by the 1983 and older historical earthquakes in the eastern margin of the Japan Sea. *Sedimentary Geology*, *135*(1–4), 1–19. https://doi.org/10.1016/S0037-0738(00)00059-2
Peakall, J., McCaffrey, W. B., & Kneller, B. (2000). A process model for the evolution, morphology and architecture of sinuous submarine channels. *Journal of Sedimentary Research*, *70*(3), 434–448. https://doi.org/10.1306/2dc4091c-0e47-11d7-8643000102c1865d
Piper, D. J. (1978). Turbidite muds and silts on deep-sea fans and abyssal plains. *Sedimentation in Submarine Canyons, Fans and Trenches*, *23*(2), 163–176.
Pope, S. B. (2000). *Turbulent flows*. Cambridge University Press.
Shepard, F. P. (1972). Submarine canyons. *Earth-Science Reviews*, *8*(1), 1–12. https://doi.org/10.1016/0012-8252(72)90032-3
Simmons, S. M., Azpiroz-Zabala, M., Cartigny, M. J., Clare, M. A., Cooper, C., Parsons, D. R., et al. (2020). Novel acoustic method provides first detailed measurements of sediment concentration structure within submarine turbidity currents. *Journal of Geophysical Research: Oceans*, *125*(5), e2019JC015904. https://doi.org/10.1029/2019jc015904
Stow, D. A. V., & Bowen, A. J. (1980). A physical model for the transport and sorting of fine-grained sediment by turbidity currents. *Sedimentology*, *27*(1), 31–46. https://doi.org/10.1111/j.1365-3091.1980.tb01156.x
Talling, P. J., Baker, M. L., Pope, E. L., Ruffell, S. C., Jacinto, R. S., Heijnen, M. S., et al. (2022). Longest sediment flows yet measured show how major rivers connect efficiently to deep sea. *Nature Communications*, *13*(1), 4193. https://doi.org/10.1038/s41467-022-31689-3
Talling, P. J., Cartigny, M. J., Pope, E., Baker, M., Clare, M. A., Heijnen, M., et al. (2023). Detailed monitoring reveals the nature of submarine turbidity currents. *Nature Reviews Earth & Environment*, *4*(9), 642–658. https://doi.org/10.1038/s43017-023-00458-1
Talling, P. J., Masson, D. G., Sumner, E. J., & Malgesini, G. (2012). Subaqueous sediment density flows: Depositional processes and deposit types. *Sedimentology*, *59*(7), 1937–2003. https://doi.org/10.1111/j.1365-3091.2012.01353.x
Tennekes, H., & Lumley, J. L. (1972). *A first course in turbulence*. MIT Press.
Thorpe, S. A. (1977). Turbulence and mixing in a Scottish loch. *Philosophical Transactions of the Royal Society of London Series A*, *286*(1334), 125–181. https://doi.org/10.1098/rsta.1977.0112
van Haren, H., Cimatoribus, A. A., Cyr, F., & Gostiaux, L. (2016). Insights from a 3-D temperature sensors mooring on stratified ocean turbulence. *Geophysical Research Letters*, *43*(9), 4483–4489. https://doi.org/10.1002/2016gl068032
van Haren, H., & Gostiaux, L. (2012). Energy release through internal wave breaking. *Oceanography*, *25*(2), 124–131. https://doi.org/10.5670/oceanog.2012.47
Warhaft, Z. (2000). Passive scalars in turbulent flows. *Annual Review of Fluid Mechanics*, *32*(1), 203–240. https://doi.org/10.1146/annurev.fluid.32.1.203
Yasuda, I., Fujio, S., Yanagimoto, D., Lee, K., Sasaki, Y., Zhai, S., et al. (2021). Estimate of turbulent energy dissipation rate using free-fall and CTD-attached fast-response thermistors in weak ocean turbulence. *Journal of Oceanography*, *77*(1), 17–28. https://doi.org/10.1007/s10872-020-00574-2
Zanuttigh, B., & Lamberti, A. (2007). Instability and surge development in debris flows. *Reviews of Geophysics*, *45*(3), RG3006. https://doi.org/10.1029/2005rg000175